[CANCER RESEARCH 62, 1315–1320, March 1, 2002]

Advances in Brief

Intratumoral Lymphangiogenesis and Lymph Node Metastasis in Head and Neck Cancer[1]

Nigel J. P. Beasley, Remko Prevo, Suneale Banerji, Russell D. Leek, John Moore, Philippe van Trappen, Graham Cox, Adrian L. Harris, and David G. Jackson[2]

Oxford Centre for Head and Neck Oncology, Radcliffe Infirmary, Oxford OX2 6HE [N. J. P. B., G. C.]; Medical Research Council Human Immunology Unit, Institute of Molecular Medicine, John Radcliffe Hospital, Headington, Oxford OX3 9DS [R. P., S. B., D. G. J.]; Imperial Cancer Research Fund Molecular Oncology Group, Institute of Molecular Medicine, John Radcliffe Hospital, Oxford OX3 9DU [R. L., J. M., A. L. H.]; Gynaecology Cancer Research Unit, St. Bartholomew's Hospital, London EC1A 7BE [P. v. T.], United Kingdom

Abstract

How tumors access and spread via the lymphatics is not understood. Although it is clear that dissemination via the blood system involves hemangiogenesis, it is uncertain whether tumors also induce lymphangiogenesis or simply invade existing peritumoral vessels. To address the issue we quantitated tumor lymph vessels in archival specimens of head and neck cancer by immunostaining for the recently described lymphatic endothelial marker LYVE-1, the vascular endothelial marker CD34, and the pKi67 proliferation marker, correlating lymph vessel density and proliferation index with clinical and pathological variables. Discrete "hotspots" of intratumoral small proliferating lymphatics were observed in all carcinomas, and a high intratumoral lymph vessel density was associated with neck node metastases ($n = 23$; $P = 0.027$) and an infiltrating margin of tumor invasion ($P = 0.046$) in the oropharyngeal subgroup. Quantitation of the lymphangiogenic growth factor vascular endothelial growth factor C by real-time PCR and immunohistochemistry revealed higher levels of mRNA in tumor tissue than in normal samples ($n = 8$; $P = 0.017$), but no obvious correlation with intratumoral lymphatics. Our results provide new evidence that proliferating lymphatics can occur in human cancers and may in some cases contribute to lymph node metastasis.

Introduction

For tumors to spread to lymph nodes, they must first invade the lymphatic system. In human cancers, it is not known whether this is achieved through the formation and invasion of new lymphatics within the tumor (tumor lymphangiogenesis) or by expansion and invasion of preexisting lymphatics at the tumor periphery (1). This issue has remained unresolved because of the difficulty in distinguishing lymphatics from blood vessels coupled with the lack of detailed knowledge concerning the molecular mechanisms of lymphangiogenesis (1, 2).

Recent studies in animals have shown that the proliferation of lymph vessels that occurs during embryogenesis and normal tissue growth is regulated by members of the VEGF[3] family and their receptors (3, 4). Indeed in mice, overexpression of VEGF-C and VEGF-D, respectively, in orthotopically transplanted MDA-435 breast carcinoma and 293EBNA fibrosarcoma, or in RIP1/Tag2-RIP1/VEGF-C transgenic mice has been shown to promote tumor lymphangiogenesis and subsequent lymph node metastases (5–7). In human cancers, however, the phenomenon of tumor lymphangiogenesis has yet to be directly demonstrated. Although VEGF-C has been detected in several different cancers and its levels in some cases shown to correlate with nodal metastasis (see, *e.g.*, Ref. 8; also reviewed in Ref 1), its direct effect on lymph vessel proliferation remains to be demonstrated (2).

One of the main obstacles to studies of tumor lymphangiogenesis has been the lack of specific markers for lymphatic endothelium. For example, VEGF receptor 3, a widely used and extremely valuable marker for lymph vessels in normal tissues, is also expressed on blood vessels within tumors (9, 10). Recently, we identified the new lymphatic marker, LYVE-1, a receptor for hyaluronan expressed on lymphatic endothelium both in normal and neoplastic tissue (11, 12). Here we have used immunohistochemistry with LYVE-1 in combination with blood vessel and cell proliferation markers to investigate lymphangiogenesis in HNSCC and its relationship to nodal metastasis and other pathological variables.

Materials and Methods

Patient Material. Archived paraffin-embedded tissue specimens from 70 previously untreated patients with HNSCC (31 with oral cavity carcinoma, 23 with oropharynx carcinoma, and 16 with larynx carcinoma) were studied. The median age was 61 years (range, 17–92 years); the group included 49 men and 21 women. Of these, 26 tumors were early stage ($T_{1/2}$) and 44 were late stage ($T_{3/4}$), 33 were N_0 at presentation and 37 had metastatic spread to the neck nodes (N_+). All had surgery as their first line of management, with some receiving postoperative radiotherapy. Specimens of complete resections rather than biopsies were selected so that both normal and tumor tissue were present on each slide. Tumors were graded as well differentiated, moderate, or poorly differentiated, and the margin of tumor invasion into surrounding normal tissue was identified as either pushing or infiltrating. The whole tumor area was examined, and the percentage area of necrosis within the tumor was determined.

Immunostaining. Four-μm sections of formalin-fixed, paraffin-embedded tissue were cut onto silanized glass slides, cleared of paraffin in Citroclear (HD Supplies, Aylesbury, United Kingdom) and rehydrated through graded alcohol baths. After a rinse in tap water, sections were incubated in 0.03% hydrogen peroxide for 15 min to inactivate endogenous peroxidases. Slides were then "pressure cooked" for 3 min in either 0.1 M Tris-HCl (pH 9.0)-2 mM EDTA for CD34 single staining or 0.1 M citrate buffer (pH 6.0) for all other staining and blocked in 10% normal human serum for 15 min.

Single Staining for LYVE-1/CD34. For the detection of lymphatic endothelium, slides were incubated (30 min) with 1:100–1:500 dilutions of rabbit polyclonal antihuman LYVE-1 antibody (11) in 20 mM Tris-HCl (pH 7.5) containing 150 mM NaCl and 5% (v/v) normal human serum (TBS), rinsed twice in the same buffer, and then developed using the HRP Envision System (DAKO, Ely, United Kingdom). For the detection of vascular endothelium, slides were incubated (60 min) with 1:100 diluted anti-CD34 monoclonal antibody Qbend 10 (DAKO) in TBS. After two rinses in the same buffer, they

Received 10/29/01; accepted 1/10/02.

The costs of publication of this article were defrayed in part by the payment of page charges. This article must therefore be hereby marked *advertisement* in accordance with 18 U.S.C. Section 1734 solely to indicate this fact.

[1] Supported by funds from the United Kingdom Medical Research Council and a project grant from the Association for International Cancer Research (Grant 00-311) to David G. Jackson, and by grants from the Imperial Cancer Research Fund to Adrian L. Harris.

[2] To whom requests for reprints should be addressed, at MRC Human Immunology Unit, Institute of Molecular Medicine, John Radcliffe Hospital, Headington, Oxford OX3 9DS, United Kingdom. E-mail: djackson@enterprise.molbiol.ox.ac.uk.

[3] The abbreviations used are: VEGF, vascular endothelial growth factor; HNSCC, head and neck squamous cell carcinoma; TBS, Tris-buffered saline; HRP, horseradish peroxidase; MVD, microvessel density; LVD, lymphatic vessel density.

were incubated with goat antimouse IgG (DAKO) for 30 min, washed, and incubated with alkaline phosphatase–anti-alkaline phosphatase complex for 30 min. The last two steps were repeated twice with 10-min incubations as described previously (13). Finally, slides were incubated (15 min) with new Fuchsin Red substrate prior to counterstaining with hematoxylin (Sigma Chemical Co., Poole, United Kingdom) and mounting with Aquamount (BDH, Poole, United Kingdom). MVD and LVD were determined in tumor vessel "hotspots", using a Chalkley point counting grid at high power (×250) by two observers as described previously (14). The mean of the vessel counts in three hotspots per section was recorded.

Double Staining for LYVE-1/CD34, LYVE-1/pKi67, or LYVE-1/Tumor Cytokeratins. Ten slides demonstrating high intratumoral LVD were selected for each double staining. Slides were first incubated with LYVE-1 antibodies (30 min), and then developed using the HRP or AP Envision Systems (DAKO), depending on the conjugate used to detect second antibody. Slides were then washed for 15 min in TBS and incubated (30–60 min) with monoclonal antibodies to CD34 (Qbend 10, 1:100 dilution; DAKO); the human epithelial cytokeratins 5, 6, 8, and 17 (monoclonal antibody MNF116, 1:60 dilution); or human pKi67 proliferation marker (monoclonal antibody MIB-1, prediluted; Immunotech, Marseilles, France), followed by development with HRP (DAKO EnVision System) conjugate in the case of MIB1 or AP (DAKO EnVision System) conjugate in the case of Qbend 10 and MNF116. Slides were then counterstained and mounted as described above.

Immunofluorescence Microscopy. To further discriminate between lymph vessels and blood vessels, paraffin sections (processed as described above) were incubated with a 1:100 dilution of antihuman CD34 monoclonal antibody Qbend 10 and polyclonal anti-LYVE-1, mixed together in TBS, prior to washing and incubating with a mixture of FITC-conjugated goat antimouse and Texas Red-conjugated goat antirabbit immunoglobulin (1:50 dilution in TBS; both from Southern Biotech). Slides were then mounted with fluorescent mounting medium (Vectashield) and viewed under a Zeiss Axioskop fluorescence microscope.

Quantitative Analysis of VEGF-C mRNA by Real-Time PCR. Transcript levels for VEGF-C were measured by quantitative real-time PCR, using the method of Holland *et al.* (15) in which the amount of amplified product is measured fluorometrically after duplex formation with a synthetic fluorescent oligonucleotide probe. The amount of fluorescent product at any given cycle within the exponential phase of PCR is proportional to the initial number of template copies. Assays were performed using TaqMan PCR core reagents, and the reactions were recorded and analyzed using an ABI Prism 7700 sequence detector equipped with a 96-well thermal cycler (Perkin-Elmer Applied Biosystems, Warrington, United Kingdom; Ref. 16).

Briefly, for isolation of total cellular RNA, samples of paired tumor and normal tissue samples from resected primary HNSCC (two oral cavity, two oropharynx, one larynx, three hypopharynx) were snap-frozen in liquid nitrogen, pulverized with a pestle and mortar, and subjected to mRNA preparation using TRI reagent (Sigma Chemical Co., Poole, United Kingdom) according to manufacturer's instructions. RNA samples (50–100 ng) were then incubated with 0.01 units of uracil *N*-glycosylase (2 min at 50°C) and reverse-transcribed in a 25-μl oligo(dT)-primed reaction at 60°C for 30 min. The cDNA templates were then subjected to a 5-min initial denaturation at 92°C prior to 40 cycles of PCR (92°C for 20 s and 62°C for 1 min, per cycle) in the presence of rTth DNA polymerase and primers spanning exons 2 and 3 of VEGF-C (forward primer, 5′-TCAAGGACAGAAGAGACTATAAAATTTGC-3′; reverse primer, 5′-ACTCCAAACTCCTTCCCCACAT-3′) or exons 2 and 3 of glyceraldehyde 3-phosphate dehydrogenase (forward primer, 5′-GAAGGTGAAGGTCG-GAGTC-3′; reverse primer, 5′-GAAGATGGTGATGGGATTTC-3′). The 137-bp VEGF-C and 226-bp glyceraldehyde 3-phosphate dehydrogenase products were quantitated with the oligonucleotide probes 5′-ATACACACCTC-CCGTGGCATGCATTG-3′ and 5′-CAAGCTTCCCGTTCTCAGCC-3′, respectively. labeled with the fluorophore 6-carboxyfluorescein at the 5′ end and the fluorescent quenching group 6-carboxytetramethylrhodamine at the 3′ end.

Statistics. Statistical analysis was carried out using the whole group of 70 patients with HNSCC as well as each subsite, the oral cavity, oropharynx, and larynx, separately. LVD was divided into two categories, high and low, by the highest third. Tumor stage was divided into two categories, early (T_1 or T_2) and advanced (T_3 or T_4), and nodal stage into N_0 (node negative at presentation) and N_+ (node positive at presentation). The associations between LVD and sex, T-stage, N-stage, grade of tumor, necrosis, and margin of invasion were examined using the Pearson χ^2 test. The correlation between LVD and MVD or VEGF-C mRNA copy number was examined using Spearman correlation. The difference in VEGF-C mRNA copy number between tumor and adjacent normal tissue samples was examined using the Wilcoxon signed-ranks test. All statistical calculations were performed using SPSS software, version 9.0.

Results

Identification of Intratumoral Lymphatics in HNSCC. To characterize lymph vessels in HNSCC, we carried out immunostaining of oral cavity, oropharyngeal, and laryngeal carcinomas with antibodies to the LYVE-1 HA receptor, previously identified as a marker for lymphatic vessel endothelium in human and murine tissues (11, 12). Numerous large, LYVE-1-reactive, irregularly shaped, thin-walled subdermal lymphatics were detected in sections of normal tongue

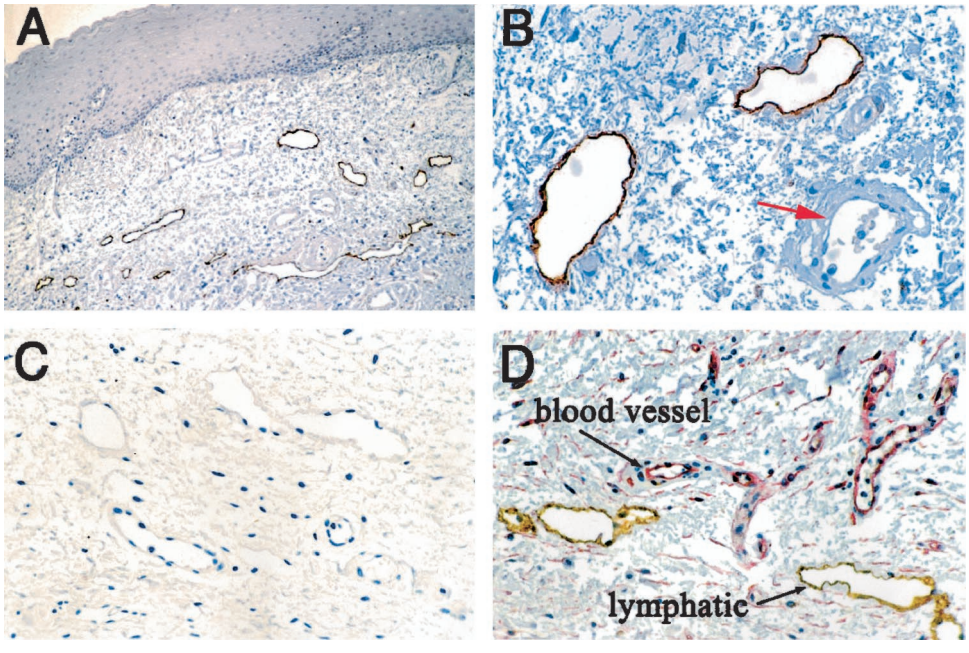

Fig. 1. Immunostaining of lymphatic vessels in normal tongue. Lymphatic vessels underlying the epithelium are positively stained with LYVE-1 antibody (*A* and *B*; magnification, ×100 in *A* and ×320 in *B*), but not with control pre-immune serum (*C*; magnification, ×200). In contrast, capillaries containing RBCs do not stain with LYVE-1 antibody (*B*, *red arrow*). In *D*, lymphatic vessels are further distinguished from blood capillaries by double immunostaining with LYVE-1 antibody (*brown*) and antibody to the blood vascular endothelial marker CD34 (*pink*; magnification, ×200).

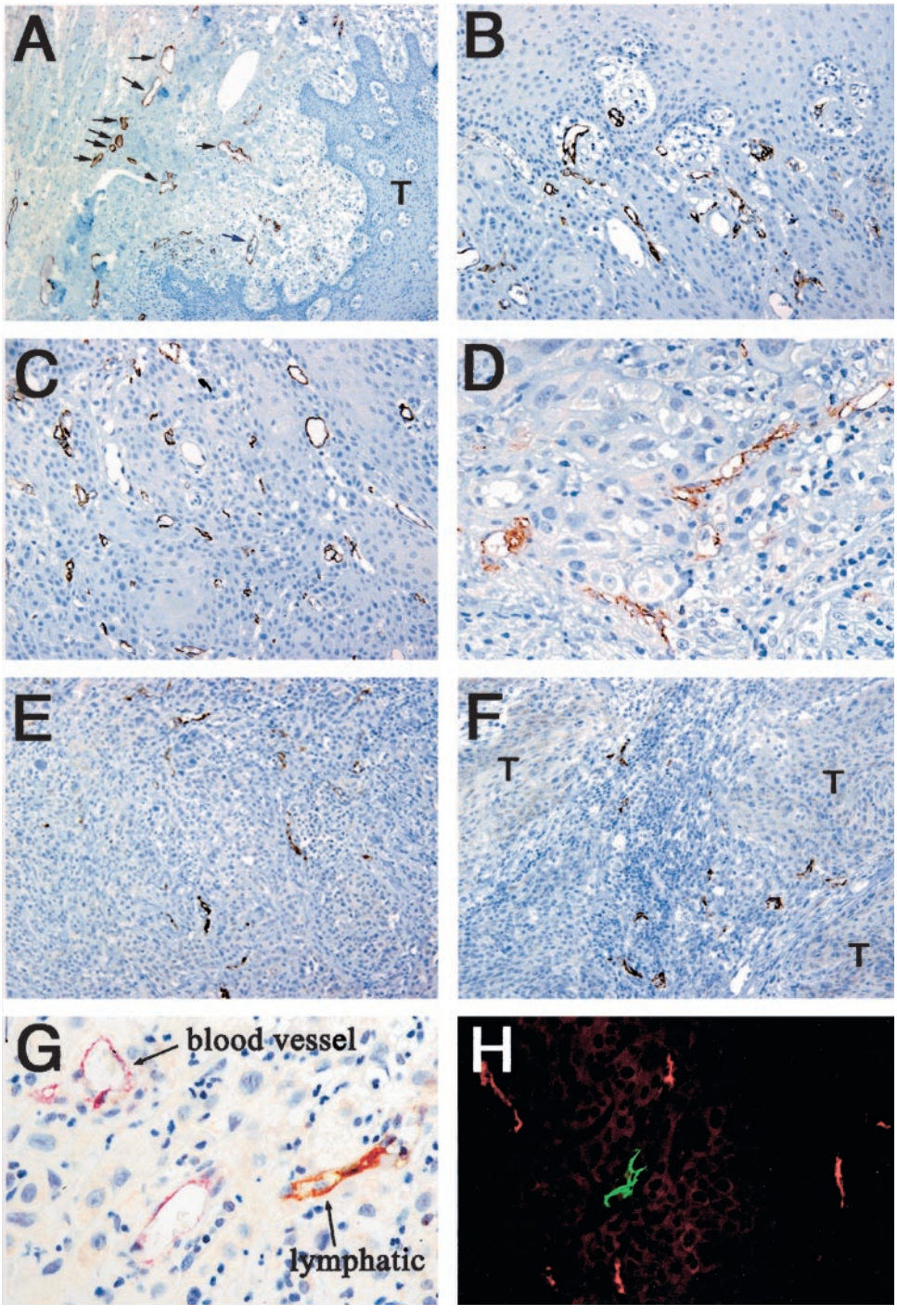

Fig. 2. Immunostaining of lymphatic vessels in squamous carcinoma of the tongue. Large, patent LYVE-1-positive lymphatic vessels (*black arrows*), some containing tumor cells (*blue arrow*), are present at the tumor margin (*A*; magnification, ×100), and smaller, multiluminal LYVE-1-positive lymphatics are present within the tumor body of carcinomas with pushing margin (*B–D*; magnification, ×200, ×200, and ×320, respectively). Small intratumoral LYVE-1-positive lymphatics are also visible interspersed between tumor foci in carcinomas with invasive margins containing leukocytic infiltrates (*E* and *F*; magnification, ×200). Tumor lymphatics are clearly distinguished from blood capillaries both by double immunohistochemical staining with LYVE-1 antibody (*brown*) and CD34 antibody (*pink*), respectively (*G*; magnification, ×400) and by double immunofluorescence staining with LYVE-1 antibody (*red*) and CD34 antibody (*green*; *panel H*; magnification, ×320). *T*, tumor.

adjacent to tumor (Fig. 1, *A* and *B*). These were clearly distinguished from adjacent blood vessels, which did not stain significantly for LYVE-1 and which were regular in shape, surrounded by smooth muscle, and contained RBCs (Fig. 1*B*). The distinction was confirmed by double immunostaining with LYVE-1 and the vascular endothelial marker CD34, which demonstrated mutually exclusive staining of the two vessel types (Fig. 1*D*). No staining was observed when preimmune serum was used as the control (Fig. 1*C*).

By comparison, HNSCC tumor areas appeared devoid of LYVE-1 +ve vessels except for the peritumoral regions, where large open lymph vessels were frequently located (Fig. 2*A* and data not shown). However, further examination revealed that intratumoral lymph vessels were in fact present, concentrated in discrete hotspots both within sheets of tumor cells in carcinomas with a pushing margin (Fig. 2, *B–D*) and in areas containing leukocyte infiltration in carcinomas with an invasive margin (Fig. 2, *E* and *F*). These intratumoral vessels often had a distinctive reticular architecture with numerous tiny or ill-defined lumina (Fig. 2, *B–G*) that differed markedly from the larger and more conventional architecture of vessels found at the tumor margin (peritumoral lymphatics; Fig. 2*A*) or within normal tissue areas (Fig. 1, *A* and *B*). Identification of the vessels as intratumoral lymphatics was confirmed by a combination of double immunohistochemical and double immunofluorescence staining with antibodies to LYVE-1 and CD34, which revealed mutually exclusive expression of these markers on the two vessel types (Fig. 2, *G* and *H*).

Proliferation Status of Intratumoral Lymphatics. The characteristic basket-like morphology of the LYVE-1-positive intratumoral lymphatics resembled the nascent structures seen in blood vessel networks during VEGF-induced hemangiogenesis *in vitro* (17), suggesting that these might be newly proliferating lymphatics. To explore this further, we carried out double immunostaining with antibodies to LYVE-1 and the proliferation-associated pKi67 nuclear protein (MIB1 antibody) to look at the occurrence of dividing nuclei among lymphatic endothelial cells within the intratumoral and peritumoral/normal lymphatic vessel populations. The results confirmed MIB1 nuclear staining in a proportion of the small intratumoral lymph vessel endothelial cells (Fig. 3, *A–D*) and, as expected, in the tumor cells themselves (see, *e.g.*, Fig. 3, *A* and *D*) and their surrounding CD34 +ve blood capillaries, (Fig. 3*E*). In contrast, no dividing nuclei were observed in either the larger peritumoral or normal tissue lymph vessel endothelia (data not shown). This evidence suggests that the intratumoral lymphatics in HNSCC are indeed proliferating new vessels and not preexisting lymphatics that had merely been surrounded and entrapped by the advancing tumor mass.

Proliferating Intratumoral Lymphatics and VEGF-C Expression. Overexpression of recombinant VEGF-C in orthotopically transplanted MDA-435 breast carcinoma and transgenic mouse insulinoma has recently been shown to induce extensive tumor lymphangiogenesis and lymph node metastasis (5, 6). To assess the possible involvement of VEGF-C in regulating intratumoral lymph vessel growth in human head and neck cancer, we compared the levels of VEGF-C mRNA in normal and tumor tissue, using quantitative real-time PCR. The results showed that the median copy number of VEGF-C mRNA was 4–5-fold higher in primary HNSCCs than in adjacent normal tissue ($n = 8$; tumor median, 9.30×10^5 (4.93×10^5–8.77×10^6; normal median, 2.21×10^5 (9.39×10^1–1.25×10^6; $P = 0.017$, Wilcoxon signed-rank test). However, there was no correlation between tumor VEGF-C mRNA copy number and intratumoral LVD in the small number of cases analyzed ($n = 8$; $P = 0.434$, Spearman correlation). In addition, preliminary staining of tumor sections with antibodies to VEGF-C detected only weak positivity throughout the tumors, and there was no evidence for elevated expression adjacent to intratumoral lymphatics (data not shown). Although these findings are far from conclusive, they indicate that there is no simple relationship between tumor VEGF-C levels and intratumoral lymph vessel proliferation in HNSCC.

Relationship of Intratumoral Lymph Vessels with Lymph Node Metastasis and Tumor Invasiveness. To assess whether intratumoral lymph vessels act as a conduit for metastasis, we looked for evidence of tumor cells within the lumen by double staining with LYVE-1 and the squamous cell cytokeratin antibody MNF116. The results revealed tumor aggregates inside some of the LYVE-1 +ve peritumoral lymphatics in each of the three HNSCC categories (Fig. 3*F* and data not shown); however, no aggregates were reliably identified within the smaller LYVE-1 +ve intratumoral vessels. Quantitation of intratumoral LVD by the Chalkley counting method revealed a statistically significant association ($P = 0.027$, Pearson's χ^2; $n = 23$; Table 1) between high intratumoral LVD (highest tertile) and lymph node metastases in oropharyngeal carcinoma, but not in oral

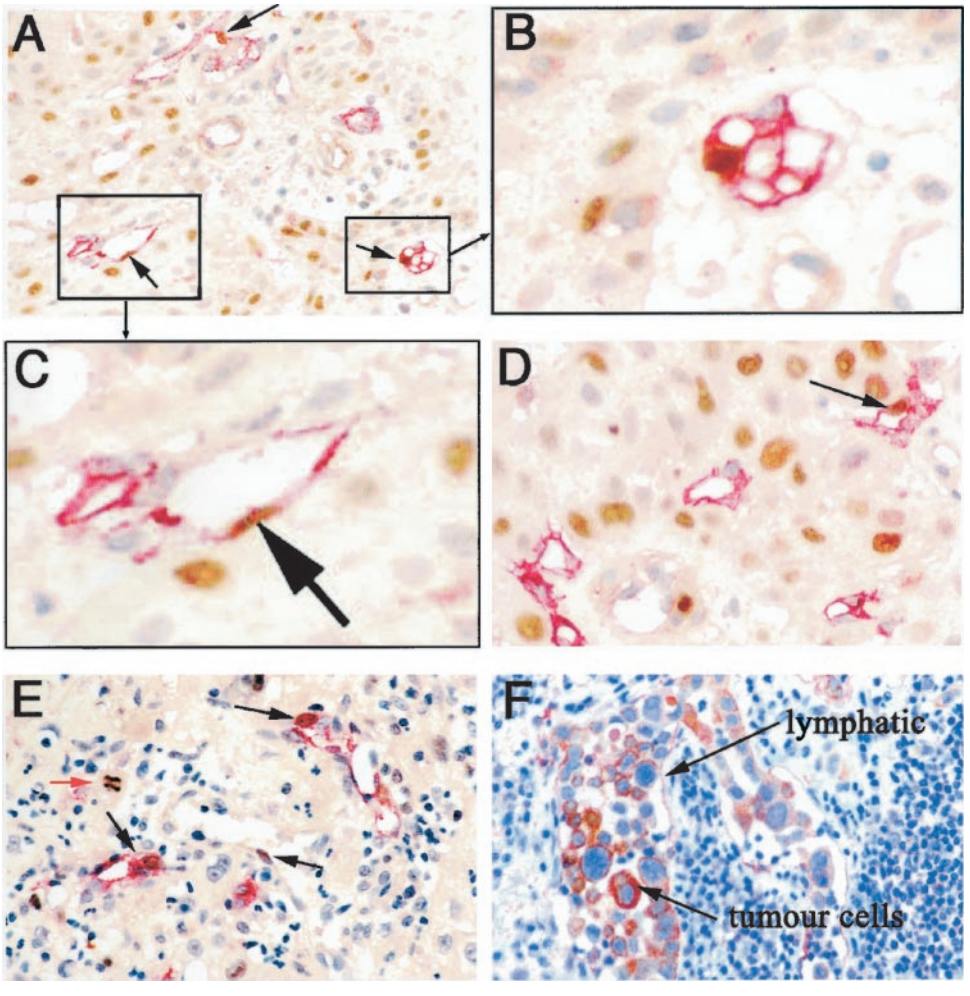

Fig. 3. Newly dividing intratumoral lymphatic vessels and blood vessels are detected by double staining for the pKi67 proliferation antigen (*brown* nuclear staining) and either LYVE-1 or CD34, respectively (*pink* membrane/cytoplasmic staining in each case). *Panels A–D* show examples of dividing LYVE-1/MIB-1 double-positive small lymph vessels (*black arrows*) surrounded by large numbers of dividing LYVE-1-negative/MIB-1-positive squamous carcinoma cells. *Panel E* shows blood capillaries containing dividing CD34/MIB-1 double-positive vascular endothelial cells (*black arrows*) and an adjacent dividing tumor cell containing a mitotic figure (*red arrow*). *Panel F* shows aggregates of cytokeratin-positive tumor cells (monoclonal antibody MNF116; *brown staining*) present within the lumen of a large LYVE-1-positive peritumoral lymphatic vessel (*pink staining*). Magnification was as follows: *panel A*, ×200; *panel B*, ×1000; *panel C*, ×1000; *panel D*, ×400; *panel E*, ×200; *panel F*, ×400.

Table 1 *Patient demographics and pathological scoring*

	LVD category,[a] *n*							
	All cases ($n = 70$)		Oral cavity ($n = 31$)		Oropharynx ($n = 23$)		Larynx ($n = 16$)	
	Low	High	Low	High	Low	High	Low	High
LVD, Median (range) (Chalkley count)	3.0 (0–3.7)	4.7 (4.0–7.3)	2.67 (0–3.7)	4.5 (4.0–5.3)	3.0 (1.0–3.7)	4.8 (4.0–6.0)	3.3 (0–3.67)	4.3 (4.0–7.3)
Sex								
M	32	17	12	5	11	6	9	6
F	11	10	9	5	2	4	0	1
T stage								
$T_{1/2}$	16	10	9	6	4	3	3	1
$T_{3/4}$	27	17	12	4	9	7	6	6
N stage								
N_0	23	10	13	8	5	0	5	2
N_+	20	17	8	2	8	10	4	5
Tumor grade (differentiation)								
Poor	4	4	1	2	1	2	2	0
Moderate	32	20	14	7	11	6	7	7
Well	7	3	6	1	1	2	0	0
Tumor margin								
Pushing	20	4	9	1	8	2	3	1
Invasive	21	23	12	9	5	8	4	6
Necrosis								
0	22	18	14	8	6	7	2	3
1	15	8	4	1	6	3	5	4
2	6	1	3	1	1	0	2	0

[a] Tertiles based on LVD category: high, highest tertile; low, lower two tertiles.

cavity carcinoma ($n = 31$) or laryngeal carcinoma ($n = 16$). These findings argue that the formation of intratumoral lymph vessels may not facilitate nodal metastasis in all types of HNSCC. Alternatively, other important factors (as yet unidentified) in addition to mere access to lymph vessels may also be required for some tumors to metastasize to lymph nodes (see "Discussion").

There was also a significant association between an infiltrating tumor margin and an intratumoral LVD in the highest tertile when all three subgroups of HNSCC were considered together ($n = 68$; $P = 0.004$, Pearson's χ^2; Table 1). Again, this was found in the oropharyngeal carcinoma subgroup ($n = 23$; $P = 0.046$, Pearson's χ^2), but not in the oral cavity carcinoma ($n = 31$) or laryngeal carcinoma subgroups ($n = 14$). Interestingly, an infiltrating tumor margin is known to be associated with increased tumor aggressiveness (18) and with neck node metastases and poor prognosis in HNSCC (19).

Finally, there was no correlation between LVD and MVD by the Spearman correlation (data not shown), and there was no significant association between LVD and sex, T-stage, grade of differentiation, or necrosis in any of the subgroups when considered alone or together (Table 1).

Discussion

The blood-borne metastasis of human cancers is known to involve invasion of intratumoral blood vessels generated by the process of tumor angiogenesis. In the case of lymph-borne metastasis, however, the occurrence and involvement of lymphangiogenesis have been demonstrated only in experimental mouse tumors (5–7) and their role in human cancers remain controversial. In this report we have demonstrated that intratumoral lymph vessel proliferation indeed occurs in HNSCCs and that in oropharyngeal carcinoma it correlates with lymph node metastasis.

The evidence that the intratumoral vessels we observed are newly proliferating rather than trapped preexisting or hyperplastic lymph vessels may be listed as follows. First, the morphology of intratumoral vessels resembles that of immature rather than mature lymphatics insofar as they have a much smaller diameter, often comprising two to three individual endothelial cells and containing multiple lumina, reminiscent of newly angiogenic blood vessels (17). Second, unlike peripheral lymph vessels and vessels close to the tumor margin, they contained proliferating nuclei. Third, they were often located in the middle of tumor sheets rather than confined to islands of stroma formed from invaginations of normal tissue. We cannot at this stage conclude whether the proliferating lymph vessels arise from bone marrow-derived precursors/lymphangioblasts (Ref 20; true lymphatic vasculogenesis) or by sprouting from co-opted peritumoral vessels (lymphangiogenesis). However, we favor the latter possibility, which would imply that the intratumoral and peritumoral vessels may well interconnect (see below). Analysis of vessel continuity in human cancer tissue by methods such as dye uptake studies (21) would, however, be difficult if not impossible to accomplish, and such studies must continue to rely on the use of animal models.

The main significance of proliferating intratumoral lymph vessels is that they could provide a possible route for the spread of HNSCC tumors to local lymph nodes. Our finding in oropharyngeal carcinoma that a high intratumoral LVD correlates with neck node metastasis supports this hypothesis and again lends credence to the possibility that the intratumoral and peritumoral lymph vessels interconnect. However, this must be balanced by our finding that laryngeal and oral cavity carcinomas displayed no correlation between LVD and nodal metastasis. Perhaps only a small number of cancers exploit intratumoral lymphatics for metastasis. In any event, the link between lymphangiogenesis/lymphoproliferation and dissemination to lymph nodes is likely to be complex. For example, the three HNSCC subgroups, although equally lymphangiogenic, may vary in their capacity to invade lymphatics. This could be attributable to differential production/activation of factors such as matrix metalloproteinases or tumor growth factor β (22, 23) or of growth factors, such as VEGF-A, that increase blood vessel (and perhaps lymph vessel) permeability (24). Future studies using RNA profiling or proteomic analyses are likely to be required to resolve these issues.

It is difficult to conclude whether proliferation of intratumoral lymph vessels in HNSCC is a consequence of VEGF-C or VEGF-D action, in a fashion analogous to that seen in recent studies with mouse tumor models (5, 7). Although VEGF-C expression was elevated in HNSCC relative to normal tissue, there was no clear correlation

between mRNA levels and intratumoral LVD or any evidence of increased VEGF-C immunoreactivity close to hotspots of proliferating lymph vessels. As in hemangiogenesis where several growth factors, including VEGFs, fibroblast growth factors, and angiopoietins, regulate vessel growth (25), multiple growth factors are also likely to regulate lymphangiogenesis. The identification of such factors will be greatly facilitated by the isolation and culture of primary lymphatic endothelial cells using markers such as LYVE-1.

Finally, although tumor emboli were occasionally observed within peritumoral vessels in all three HNSCC subtypes, they were not obvious within intratumoral vessels. These findings indicate that intratumoral lymph vessels are probably not a major conduit for nodal metastasis in HNSCC. However, it should be appreciated that there are limitations in detecting what may be rare events by examining small sections of archival tissue at a single point in time. We therefore speculate that the spread of HNSCC tumor cells to lymph node may involve invasion of both peritumoral and intratumoral vessels. Indeed it is possible that some of the emboli we observed within peritumoral vessels originate from initial invasion of intratumoral vessels. Such speculation seems reasonable in light of reports in the mouse that the intratumoral lymphatics of VEGF-C- and VEGF-D-transfected tumors frequently contained intralumenal emboli (5, 7). Blockade of tumor lymphangiogenesis or intralymphatic invasion may therefore be an option for future therapeutic intervention in some types of human cancer.

Acknowledgments

We thank Professor Kari Alitalo, Molecular/Cancer Biology Laboratory, Haartman Institute, University of Helsinki (Helsinki, Finland), for kindly providing polyclonal antibody to VEGF-C.

References

1. Pepper, M. S. Lymphangiogenesis and tumor metastasis: myth or reality? Clin. Cancer Res., *7:* 462–468, 2001.
2. Jackson, D. G. New markers for the study of lymphangiogenesis. Anticancer Res., *7:* 1–5, 2001.
3. Oh, S. J., Jeltsch, M. M., Birkenhager, R., McCarthy, J. E., Weich, H. A., Christ, B., Alitalo, K., and Wilting, J. VEGF and VEGF-C: specific induction of angiogenesis and lymphangiogenesis in the differentiated avian chorioallantoic membrane. Dev. Biol., *188:* 96–109, 1997.
4. Jeltsch, M., Kaipainen, A., Joukov, V., Meng, X., Lakso, M., Rauvala, H., Swartz, M., Fukumura, D., Jain, R. K., and Alitalo, K. Hyperplasia of lymphatic vessels in VEGF-C transgenic mice. Science (Wash. DC), *276:* 1423–1425, 1997.
5. Skobe, M., Hawighorst, T., Jackson, D. G., Prevo, R., Janes, L., Velasco, P., Riccardi, L., Alitalo, K., Claffey, K., and Detmar, M. Induction of tumor lymphangiogenesis by VEGF-C promotes breast cancer metastasis. Nat. Med., *7:* 192–198, 2001.
6. Mandriota, S. J., Jussila, L., Jeltsch, M., Compagni, A., Baetens, D., Prevo, R., Banerji, S., Huarte, J., Montesano, R., Jackson, D. G., Orci, L., Alitalo, K., Christofori, G., and Pepper, M. S. Vascular endothelial growth factor-C-mediated lymphangiogenesis promotes tumour metastasis. EMBO J., *20:* 672–682, 2001.
7. Stacker, S. A., Caesar, C., Baldwin, M. E., Thornton, G. E., Williams, R. A., Prevo, R., Jackson, D. G., Nishikawa, S., Kubo, H., and Achen, M. G. VEGF-D promotes the metastatic spread of tumor cells via the lymphatics. Nat. Med., *7:* 186–191, 2001.
8. Ohta, Y., Shridhar, V., Bright, R. K., Kalemkerian, G. P., Du, W., Carbone, M., Watanabe, Y., and Pass, H. I. VEGF and VEGF type C play an important role in angiogenesis and lymphangiogenesis in human malignant mesothelioma tumours. Br. J. Cancer, *81:* 54–61, 1999.
9. Partanen, T. A., Alitalo, K., and Miettinen, M. Lack of lymphatic vascular specificity of vascular endothelial growth factor receptor 3 in 185 vascular tumors. Cancer (Phila.), *86:* 2406–2412, 1999.
10. Valtola, R., Salven, P., Heikkila, P., Taipale, J., Joensuu, H., Rehn, M., Pihlajaniemi, T., Weich, H., deWaal, R., and Alitalo, K. VEGFR-3 and its ligand VEGF-C are associated with angiogenesis in breast cancer. Am. J. Pathol., *154:* 1381–1390, 1999.
11. Banerji, S., Ni, J., Wang, S. X., Clasper, S., Su, J., Tammi, R., Jones, M., and Jackson, D. G. LYVE-1, a new homologue of the CD44 glycoprotein, is a lymph-specific receptor for hyaluronan. J. Cell Biol., *144:* 789–801, 1999.
12. Prevo, R., Banerji, S., Ferguson, D. J., Clasper, S., and Jackson, D. G. Mouse LYVE-1 is an endocytic receptor for hyaluronan in lymphatic endothelium. J. Biol. Chem., *276:* 19420–19430, 2001.
13. Cordell, J. L., Falini, B., Erber, W. N., Ghosh, A. K., Abdulaziz, Z., MacDonald, S., Pulford, K. A., Stein, H., and Mason, D. Y. Immunoenzymatic labeling of monoclonal antibodies using immune complexes of alkaline phosphatase and monoclonal anti-alkaline phosphatase (APAAP complexes). J. Histochem. Cytochem., *32:* 219–229, 1984.
14. Fox, S. B. Tumour angiogenesis and prognosis. Histopathology, *30:* 294–301, 1997.
15. Holland, P., Abrahamson, R., Watson, R., and Gelfand, D. Detection of specific polymerase chain reaction products by utilising the 5′-3′ exonuclease activity of *Thermus aquaticus* DNA polymerase. Proc. Natl. Acad. Sci. USA, *88:* 7276–7280, 1991.
16. Heid, C., Stevens, J., Livak, K., and Willams, P. Real time quantitative PCR. Genome Res., *6:* 986–994, 1996.
17. Pettersson, A., Nagy, J. A., Brown, L. F., Sundberg, C., Morgan, E., Jungles, S., Carter, R., Krieger, J. E., Manseau, E. J., Harvey, V. S., Eckelhoefer, I. A., Feng, D., Dvorak, A. M., Mulligan, R. C., and Dvorak, H. F. Heterogeneity of the angiogenic response induced in different normal adult tissues by vascular permeability factor/vascular endothelial growth factor. Lab. Investig., *80:* 99–115, 2000.
18. Crissman, J. D. Tumor-host interactions as prognostic factors in the histologic assessment of carcinomas. Pathol. Annu., *21:* 29–52, 1986.
19. Odell, E. W., Jani, P., Sherriff, M., Ahluwalia, S. M., Hibbert, J., Levison, D. A., and Morgan, P. R. The prognostic value of individual histologic grading parameters in small lingual squamous cell carcinomas. The importance of the pattern of invasion. Cancer (Phila.), *74:* 789–794, 1994.
20. Papoutsi, M. Tomarev, S. I. Eichmann, A. Prols, F. Christ, B. Wilting, J. Endogenous origin of the lymphatics in the avian chorioallantoic membrane. Dev. Dyn., *222:* 238–251, 2001.
21. Leu, A. J., Berk, D. A., Lymboussaki, A., Alitalo, K., and Jain, R. K. Absence of functional lymphatics within a murine sarcoma: a molecular and functional evaluation. Cancer Res., *60:* 4324–4327, 2000.
22. Bergers, G., Brekken, R., McMahon, G., Vu, T. H., Itoh, T., Tamaki, K., Tanzawa, K., Thorpe, P., Itohara, S., Werb, Z., and Hanahan, D. Matrix metalloproteinase-9 triggers the angiogenic switch during carcinogenesis. Nat. Cell Biol., *2:* 737–744, 2000.
23. Maehara, Y., Kakeji, Y., Kabashima, A., Emi, Y., Watanabe, A., Akazawa, K., Baba, H., Kohnoe, S., and Sugimachi, K. Role of transforming growth factor-β1 in invasion and metastasis in gastric carcinoma. J. Clin. Oncol., *17:* 607–614, 1999.
24. Dvorak, H. F., Nagy, J. A., Feng, D., Brown, L. F., and Dvorak, A. M. Vascular permeability factor/vascular endothelial growth factor and the significance of microvascular hyperpermeability in angiogenesis. Curr. Top. Microbiol. Immunol., *237:* 97–132, 1999.
25. Yancopoulos, G. D., Davis, S., Gale, N. W., Rudge, J. S., Wiegand, S. J., and Holash, J. Vascular-specific growth factors and blood vessel formation. Nature (Lond.), *407:* 242–248, 2000.